Estuarine, Coastal and Shelf Science 329 (2026) 109605

Contents lists available at ScienceDirect

Estuarine, Coastal and Shelf Science

journal homepage: www.elsevier.com/locate/ecss

Climatic forcing modulates non-stationary environmental synchrony in shellfish production regions

Carlos Lara [a,b], Richard Muñoz [a,c], Sebastián I. Vásquez [c,d], Felipe I. Torres [e,f], Amalia M.S. Detoni [f], Bernardo R. Broitman [f,g], Bernard Cazelles [h,i,*]

[a] Departamento de Ecología, Facultad de Ciencias, Universidad Católica de la Santísima Concepción, Concepción, Chile
[b] Centro de Investigación en Recursos Naturales y Sustentabilidad, Universidad Bernardo O'Higgins, Santiago, Chile
[c] Programa de Doctorado en Oceanografía, Universidad de Concepción, Concepción, Chile
[d] Instituto de Investigación Pesquera, Talcahuano, Chile
[e] Programa de Doctorado en Ciencias Mención Biodiversidad y Biorecursos, Universidad Católica de la Santísima Concepción, Concepción, Chile
[f] Instituto Milenio en Socio-Ecología Costera (SECOS), Santiago, Chile
[g] Departamento de Ciencias, Facultad de Artes Liberales, Universidad Adolfo Ibáñez, Viña Del Mar, Chile
[h] IBENS, UMR CNRS 8197, Eco-Evolution Mathématique, Ecole Normale Supérieure, Paris, France
[i] MUSCLEES, Centre INRIA de Paris, Paris, France

ARTICLE INFO

Keywords:
Multiscale fluctuations
Transient association
Satellite data
Partial wavelet coherence
Empirical orthogonal function

ABSTRACT

Coupled fluctuations between ecological and environmental processes — i.e., synchrony — have been documented in marine ecosystems across multiple spatial and temporal scales. To investigate multiscale synchrony, we applied Wavelet Coherence (WC) and Partial Wavelet Coherence (PWC) analyses to disentangle nonstationary associations between local and regional environmental variables that are critical for shellfish aquaculture along the southeastern Pacific. Specifically, we examined and controlled the effects of local associations between sea surface temperature (SST) and shellfish food supply, represented by normalized fluorescence line height ($nFLH$), in relation to the regional El Niño–Southern Oscillation ($ENSO$). Using MODIS-Aqua satellite time series (2003–2022) and the Multivariate ENSO Index (MEI), we assessed temporal changes in the coupling between SST and $nFLH$ in two bivalve aquaculture regions: Tongoy Bay (north-central Chile) and northern Chiloé (southern Chile). Our analyses revealed that SST exhibited a stationary annual cycle explaining over 95% of total variance, while $nFLH$ showed a dominant annual mode accounting for more than 60% of variance. However, the second mode of $nFLH$ in both Tongoy Bay and northern Chiloé reflected the influence of local drivers — such as freshwater discharge events — that were not synchronized with the dominant pattern. PWC analyses identified significant intra- and interannual synchrony between $nFLH$ and $ENSO$ within the 1.5–2.5 yr and 3–5 yr bands, after removing the influence of SST. These results demonstrate that large-scale climatic forcing modulates local environmental synchrony through differential regional coupling strengths. Consequently, the predictability of environmental conditions relevant to shellfish aquaculture in both regions appears to be strongly constrained by $ENSO$-driven variability operating across multiple temporal scales.

1. Introduction

Over the past two decades, remote sensing has enabled the study of time-varying environmental processes over large spatial scales, unraveling the basic dynamics and drivers of biospheric processes (Behrenfeld et al., 2009; Duveiller et al., 2018; Stramski et al., 2022; Sundararaman and Shanmugam, 2024). Climatic-scale biophysical synchrony (henceforth, synchrony) are temporal changes in biological processes unfolding together with environmental drivers over entire basins or continents (Bjørnstad et al., 1999; Hansen et al., 2020). These coupled quasi-periodic patterns have been observed in terrestrial (Defriez and Reuman, 2017b; Tsang et al., 2023) and marine (Thackeray et al., 2010; Batchelder et al., 2012; Buttay et al., 2017; Defriez and Reuman, 2017b,a) ecosystems. One of the most common mechanisms driving synchrony is the Moran effect. Moran-type processes are usually linked to disturbances driven by large-scale processes, i.e. changes in the

* Corresponding author at: IBENS, UMR CNRS 8197, Eco-Evolution Mathématique, Ecole Normale Supérieure, Paris, France.
E-mail address: cazelles@biologie.ens.fr (B. Cazelles).

https://doi.org/10.1016/j.ecss.2025.109605
Received 27 August 2025; Received in revised form 2 November 2025; Accepted 3 November 2025
Available online 28 November 2025
0272-7714/© 2025 Published by Elsevier Ltd.

seasonal pattern of sea surface temperature (SST) following El Niño–Southern Oscillation (ENSO) events or the different phases of the Pacific Decadal Oscillation (PDO). These random and spatially autocorrelated environmental processes trigger changes in ecosystem dynamics that ripple across space and time (Defriez and Reuman, 2017b,a; Sheppard et al., 2019). Moran-type coupled oscillations are incorporated into population dynamics through strongly conserved eco-evolutionary patterns such as phenology or reproductive cycles. For example, global terrestrial vegetation and ocean phytoplankton biomass are synchronized with temperature, precipitation, and SST, respectively, over multiple temporal scales (Defriez and Reuman, 2017b). In this way, global-scale biogeophysical drivers of synchrony and their ecosystem-level consequences are well understood for mechanisms operating over long time scales. By implication, since climatic-scale synchrony in biological productivity is regulated through predictable physical mechanisms, ongoing climatic change is disrupting the temporal structure of environmental processes. Moreover, the changing climate is poised to alter the structure, stability, and functioning of ecosystems in regions under dynamical environmental forcing, such as highly productive coastal regions (Walter et al., 2024; Wanner et al., 2024).

Rapid growth of the human population, rising CO_2 emissions, limited land, and the demand for high-quality protein and fatty acids will challenge current food production systems (Ezgeta-Balić et al., 2012; Ottinger et al., 2016; Boyd et al., 2022). Shellfish aquaculture, a sustainable and highly efficient food production system, constitutes approximately 45% of global aquaculture production and it is projected to increase to 53% by 2050 (FAO, 2020). In this context, understanding how a changing climate can impact biological productivity via Moran-type processes is crucial for aquaculture (Reid et al., 2019; Lara et al., 2016). Recent studies suggest that in mid- and high-latitude ecosystems, rising SST and changing phytoplankton patterns are affecting the physiological performance and larval supply of bivalves over continental scales (Philippart et al., 2003; Maulu et al., 2021). These biological impacts may lead to changes in the distribution and amount of habitats suitable for bivalve cultivation (Froehlich et al., 2018; Torres et al., 2025), threatening global food security. The Humboldt Current Ecosystem, flowing along the coast of southern South America, displays extraordinary primary and secondary productivity accounting for almost 20% of global fisheries landings (FAO, 2020; Chavez and Messié, 2009). The elevated primary productivity also sustains a large shellfish aquaculture industry, Chile is among the top global producers of farmed mussels and scallops (FAO, 2020; Torres et al., 2025). Marine shellfish production in Chile, as elsewhere, is largely based on open water aquaculture, hence completely dependent on marine productivity: cultivated species are filter-feeders and seedstock replenishment depends on the capture of wild larvae (Molinet et al., 2025; von Brand et al., 2016). Remotely detected surface characteristics — SST, $Chla$ — have been used to approximate the suitability of the habitat of shellfish (Snyder et al., 2017; Newell et al., 2021). On the other hand, local, non-stationary changes in phytoplankton biomass have been also related to variations in nutrient concentration, salinity or turbidity (Jiang et al., 2014; Abbate et al., 2017; Ferreira et al., 2020; Poblete-Ulloa et al., 2024). The latter can be approximated though a remotely-sensed proxy of phytoplankton physiological state, normalized Fluorescence Line Height ($nFLH$, (Behrenfeld et al., 2009)), but rarely used to examine conditions for aquaculture. When coupled to extended *in situ* measurements on the suite of factors that can impact aquaculture, remote sensing products cant allow the identification of climate impacts. However, such *in situ* datasets are largely unavailable in the part of the Humboldt Current Ecosystem where shellfish aquaculture is carried out (Ramajo et al., 2020; Saavedra et al., 2020). Following their tight coupling over multiple temporal scale to phytoplankton dynamics, satellite-derived SST measurements are routinely used as an indicator of low-frequency climate forcing by ENSO or PDO on $chla$ (Barrows et al., 2007; Martinez et al., 2009). In this way, changes in SST provide a mechanistic linkage to habitat suitability for farmed bivalves (Boyd et al., 2022), and an indication of first-order changes in phytoplankton biomass that may be associated to large-scale climatic forcing (Martinez et al., 2009; Kahru et al., 2012; Weidberg et al., 2020).

As discussed above, time series from natural ecosystems are typically noisy, non-stationary, and exhibit complex behaviors (Cazelles and Stone, 2003; Cazelles, 2004). Shellfish aquaculture along the Humboldt Current Ecosystem is fully dependent on the interplay between seasonal and sub-seasonal processes that interact with nonlinear forcing over longer temporal scales (Lara et al., 2016; Ramajo et al., 2020; Broitman et al., 2022). Linear correlations of short time series have shown that coupled inter-annual variation in SST and phytoplankton biomass (measured as satellite surface chlorophyll-a), likely in association to climatic forcing, can severely curtail larval supply for aquaculture (Lara et al., 2016; Broitman et al., 2022). Such disruptions pose significant challenges for the sustainability of this important socio-ecological system (Broitman et al., 2017). Wavelets are increasingly used to associate organismal responses to multiple environmental processes taking place at different frequencies by detecting transient and multiscale relationships (Cazelles et al., 2007). To this end, we used wavelet coherence analyses and partial wavelet coherence (PWC) to determine associations between ocean satellite-derived times series of biophysical drivers of aquaculture productivity. This study aims to (1) describe and compare the temporal synchrony patterns in key bio-oceanographic characteristics and (2) disentangle the impact of global climate ($ENSO$) in multiscale synchrony in primary biological measured as satellite $nFLH$, as a proxy of food supply for shellfish, and SST, a primary indicator of physical processes controlling primary and secondary productivity in the main aquaculture zones of Chile.

2. Materials and methods

2.1. Study area

Two regions of the Chilean coast account for almost the totality of exported shellfish and together the represent 5% of the world total (Fig. 1A), making Chile the second-largest producer after China, which accounts for 76% of the total (FAO, 2025). The first zone is Tongoy Bay, located on the semiarid coast of northern-central Chile (Fig. 1B). It is a small equator-facing Bay sheltered from upwelling-favorable winds by a large headland (Punta Lengua de Vaca, PLV), which closes the Bay to the southwest. The PLV headland is the largest upwelling center of the northern-central section of the coastline (Bravo et al., 2016; Lagos et al., 2016). Aquaculture in Tongoy Bay is primarily focused on the Peruvian Bay scallop *Argopecten purpuratus* and accounts for 90% of the total scallop production in Chile (Bakit et al., 2023). The second (Fig. 1C) shellfish producing zone is focused on the Chilean mussel *Mytilus chilensis*. It occupies an area much larger than Tongoy bay in southern Chile, northern Patagonia characterized by high heterogeneity in local environmental conditions such as chlorophyll-*a*, SST and freshwater input (Iriarte et al., 2007; Saldías et al., 2021; Flores et al., 2022; Muñoz et al., 2023).

2.2. Satellite ocean color data and climatic index

High spatial resolution daily data on surface normalized fluorescence line height ($nFLH$, W m^{-2} μm^{-1} sr^{-1}) and sea surface temperature (SST) from the Moderate Resolution Imaging Spectroradiometer (MODIS, onboard Aqua) were used to characterize the temporal variation in environmental surface characteristics in the study areas from 2003 to 2022. The MODIS L2 data were obtained from NASA's ocean color website (http://oceancolor.gsfc.nasa.gov, accessed on September 5, 2023). Standard procedures, including atmospheric corrections, were used for satellite estimates (O'Reilly et al., 2000). The quality-controlled daily swaths were processed to generate gridded monthly composites at a 1 km spatial resolution. From these composites, univariate monthly time series were derived by computing the spatial average

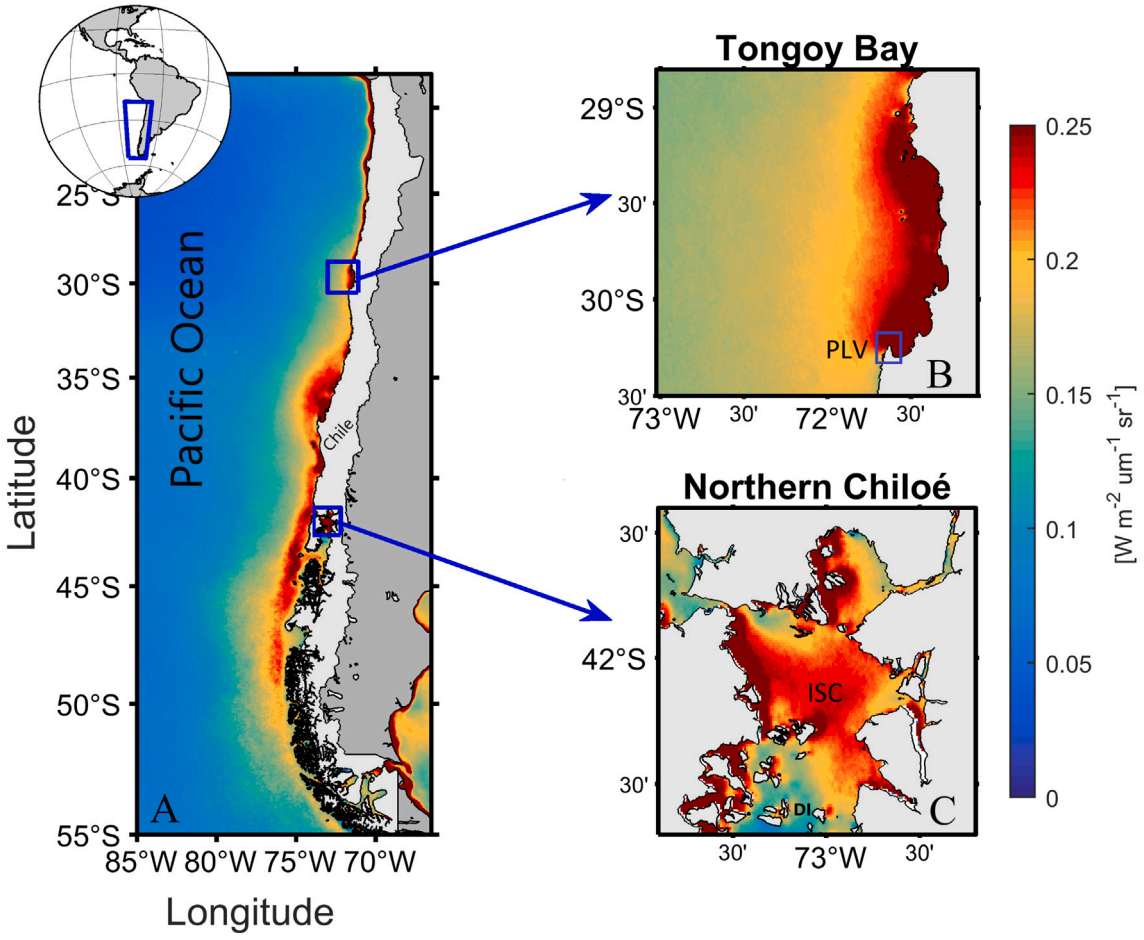

Fig. 1. Study area. Normalized fluorescence line height ($nFLH$; W m^{-2} μm^{-1} sr^{-1}) in (A) coastal Chile (18–55°S), (B) Tongoy Bay, (C) Northern Chiloé. PLV: Punta Lengua de Vaca, ISC: Inner Sea of Chiloé, DI: Desertores Islands.

at each selected location. These time series were subsequently used to analyze the temporal variability of the satellite-derived environmental conditions.

We used the Multivariate ENSO Index Version 2 (MEI v2) in a wavelet analysis to assess the coherence between the $ENSO$ pattern of ocean–atmosphere variability across the Pacific basin and local environmental variables (FLH and SST) in Tongoy Bay and northern Chiloé. The MEI time series corresponds to the leading combined Empirical Orthogonal Function (EOF) of sea level pressure, sea surface temperature (SST), the zonal and meridional components of surface wind and outgoing longwave radiation, with all the variables averaged over the 30° S–30° N and 100° E–70° W region (https://psl.noaa.gov/enso/mei/, accessed 23 July 2023).

A schematic of the workflow for the analysis of MODIS-Aqua satellite data is shown in (Fig. 2). Level-2 data are processed to Level-3 to obtain sea surface temperature (SST) and normalized Fluorescence Line Height ($nFLH$) variables. Subsequently, preprocessing is performed through detrending and normalization. Data are analyzed using two complementary approaches: (1) Empirical Orthogonal function analysis (EOF), to identify dominant spatial modes (Modes 1 and 2) and their corresponding eigenvalues; and (2) Wavelet analysis, to decompose temporal signals and extract their periodic components in the time–frequency domain. Finally, Partial Wavelet Coherence is applied to assess the association between two signals while controlling for the influence of a third one. The details of these analyses are described in the following sections.

Empirical Orthogonal Function (EOF) analysis

We used EOF analysis to characterize the dominant patterns of spatio-temporal variability in SST, and $nFLH$. Due to the high spatial resolution of the images, we computed the EOF using Singular Value Decomposition (SVD) to avoid a very large covariance matrix (Thomson and Emery, 2014). The first and second modes captured most of the variance, so we present their temporal evolution and use the climatology of each mode to describe the monthly spatial pattern. The spatial variability patterns of the dominant modes are shown together with maps of the percentage of data in the EOF analysis. The percentage of data was calculated as: valid data points pixel/total of data pixel (2003–2022) x 100.

Time–frequency wavelet and wavelet coherence analysis

Ecological time series are recognized as non-stationary due to a complex combination of factors that modify them and make them difficult to predict both in time and space (Cazelles et al., 2008; Liu et al., 2022). Continuous wavelets allow us to quantify the various periodic components of a time series locally in time and to examine their temporal evolution (Cazelles et al., 2008, 2023). The continuous wavelet transform of a time series $x(t)$ is defined as:

$$W_x(a,\tau) = \frac{1}{\sqrt{a}} \int_{-\infty}^{\infty} x(t)\psi^* \left(\frac{t-\tau}{a}\right) dt \quad (1)$$

where ψ denotes the mother wavelet, $W_x(a,\tau)$ is the contribution of the scale, a to the signal at different positions, τ and * denote the

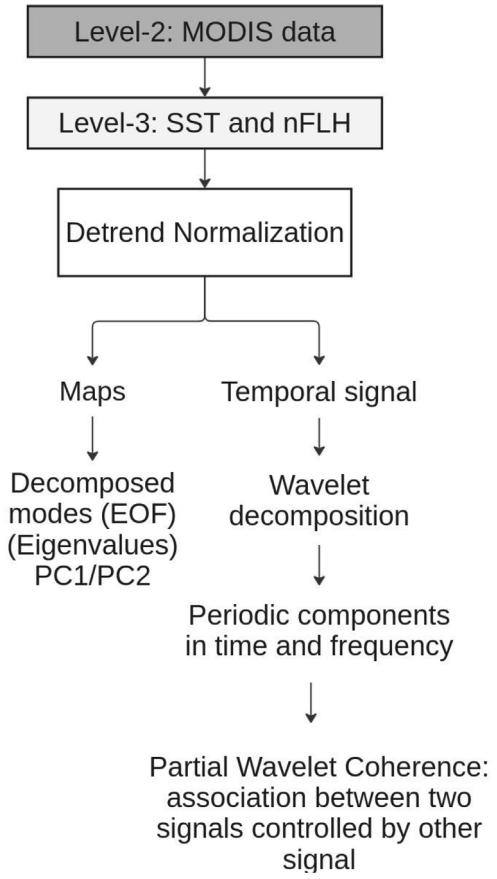

Fig. 2. Workflow diagram summarizing the analysis of MODIS-Aqua satellite data for SST and $nFLH$.

complex conjugate form (Cazelles et al., 2007, 2023). As ψ, we used the continuous Morlet wavelet, widely used in the study of ecological time series studies (Lara et al., 2019a; Xiao et al., 2019; Lara et al., 2019b). The mother Wavelet is defined as:

$$\psi(t) = \pi^{-1/4} exp(-i\omega_0 t) exp(-t^2/2) \tag{2}$$

where ω_0 is the central angular frequency of the wavelet and $\pi^{-1/4}$ a normalization factor (Cazelles et al., 2007). With the Morlet wavelet and $\omega_0 = 2\pi$, the wavelet scale a is inversely proportional to the central frequency of the wavelet, thus $a \approx 1/f$ (Cazelles et al., 2007, 2008). By analogy to Fourier analysis, the wavelet power spectrum (WPS) can be computed as $S_x(f,t) = \|W_x(f,t)\|^2$ to quantify the contribution of different periodic components to the variance along the time axis.

To analyze the statistical co-variation at a particular period between two nonstationary time series, $x_1(t)$ and $x_2(t)$, we used a Wavelet Coherence (WC):

$$WC_{x_1,x_2}(f,t) = \left(\frac{| < W_{x_1,x_2}(f,t) > |^2}{| < W_{x_1}(f,t) > | . | < W_{x_2}(f,t) > |} \right)^{1/2} \tag{3}$$

where <> denotes a smoothing operator in both time and frequency domains and $W_{x_1,x_2}(f,t)$ is the co-wavelet spectrum between $x_1(t)$ and $x_2(t)$. When $WC_{x_1,x_2}(f,t) = 1$, the two times series $x_1(t)$ and $x_2(t)$ are in perfect synchrony, and when these two times series are independent $WC_{x_1,x_2}(f,t) = 0$ (Cazelles et al., 2007, 2023). Often in ecology, local environmental signatures are modulated by regional and/or global processes (Ghil et al., 2002; Cazelles et al., 2023). To remove the effect of external variables on the relationship between the $x_1(t)$ and $x_2(t)$ time series, we applied partial wavelet coherence (PWC) (Lara et al., 2019a; Cazelles et al., 2023). PWC is based on the spectral matrix $\mathbf{\Sigma}(f,t)$ where all elements are the cross-wavelet spectrum for the i and j signals from the n time series analyzed $x_n(t)$:

$$\mathbf{\Sigma}(f,t) = \begin{pmatrix} W_{11}(f,t) & W_{12}(f,t) & \dots & W_{1n}(f,t) \\ W_{21}(f,t) & W_{21}(f,t) & \dots & W_{2n}(f,t) \\ \vdots & \vdots & \ddots & \vdots \\ W_{n1}(f,t) & W_{n2}(f,t) & \dots & W_{nn}(f,t) \end{pmatrix} \tag{4}$$

Finally, the PWC between $x_k(t)$ and $x_l(t)$, by excluding the effects of all other signals of $x_i(t)$ is defined as :

$$PWC_{kl|(\backslash kl)}(f,t) = \left(\frac{|S^{kl}(f,t)|^2}{|S^{kk}(f,t)|.|S^{ll}(f,t)|} \right)^{1/2} \tag{5}$$

where S^{kl} is the (k,l) element of the inverse spectral matrix $\mathbf{\Sigma}(f,t)^{-1}$ and $(\backslash kl)$ means all elements of $\mathbf{\Sigma}(f,t)^{-1}$ excluding the kth and the lth elements (Lara et al., 2019a; Cazelles et al., 2023).

3. Results

3.1. Temporal variability in bio-oceanographic characteristics

We used EOF analysis to characterize the spatio-temporal variability of satellite-derived ocean parameters in Tongoy Bay and northern Chiloé. Fig. 3 shows the principal temporal components of the EOF analysis for SST and $nFLH$, represented by mode 1 and 2.

In Tongoy Bay, mode 1 SST accounted for 96.79% of the total variance and was mainly associated with the annual temperature cycle and mode 2 only 3.20% (Fig. 3A, E). The spatial pattern of mode 1 shows a stronger annual cycle offshore, particularly between longitudes -72° W and -73° W. Along the coast, the annual signal showed lower intensity, which is consistent with the influence of local coastal processes such as coastal upwelling. The mode 2 spatial pattern shows a longitude gradient, with positive values nearshore and negative values offshore (Fig. 4B, C). The variability of $nFLH$ was mainly explained by mode 1 (66.05%), while mode 2 represented a greater variance than for SST with values of 33.94% (Fig. 3B,F). The spatial variability in mode 1 for $nFLH$ showed a negative coastal band that intensified north of Tongoy bay (29°20'S; 29°40'S), while a positive maximum was identified near the coast around 29° S. Mode 2 maintained the negative coastal band but with a reduced spatial extent compared to mode 1 (Fig. 4E, F). The percentage of data used in the EOF analysis for SST and $nFLH$ exceeded 98% in each pixel for the 2003–2022 period (Fig. 4A, D).

In northern Chiloé, SST mode 1 accounted for 93.56% of the variance, while mode 2 accounted for 6.43% of the total variance. The climatology of SST mode 1 was positive during austral summer and negative during austral winter, associated with the annual cycle (Fig. 3E, G). The variance explained by mode 1 of $nFLH$ (73.8%) was higher, while mode 2 explained less than <27% of the total variability. The climatology showed a negative maximum during austral winter, which decreased in summer (Fig. 3D, H). The climatology for $nFLH$ showed positive monthly averages with the exception of October (Fig. 3 H). Using more than 80% each pixel for the 2003–2022 period (Fig. 5A, D), the spatial pattern of mode 1 for SST showed maxima along the continental margin, decreasing southward as a meridional gradient toward Chiloé Island, with minima confined to the southern Desertores Islands. Mode 2 revealed marked seasonal variability between the continental margin and Chiloé Island (Fig. 5B, C). The spatial patterns of modes 1 and 2 for $nFLH$ displayed a pronounced negative core around the Desertores Islands, while the continental margin remained positive in both modes (Fig. 5E, F).

The WPS analysis showed that the temporal variability in SST in both Tongoy Bay (Fig. 6A) and northern Chiloé (Fig. 6B) was completely dominated by the annual cycle. The WPS for $nFLH$ for Tongoy Bay showed a pattern similar to SST (Fig. 7A). In northern Chiloé, the WPS for $nFLH$ was characterized by a non-stationary annual signal and its significance was interrupted during 2011–2012 and 2017–2018 (Fig. 7B).

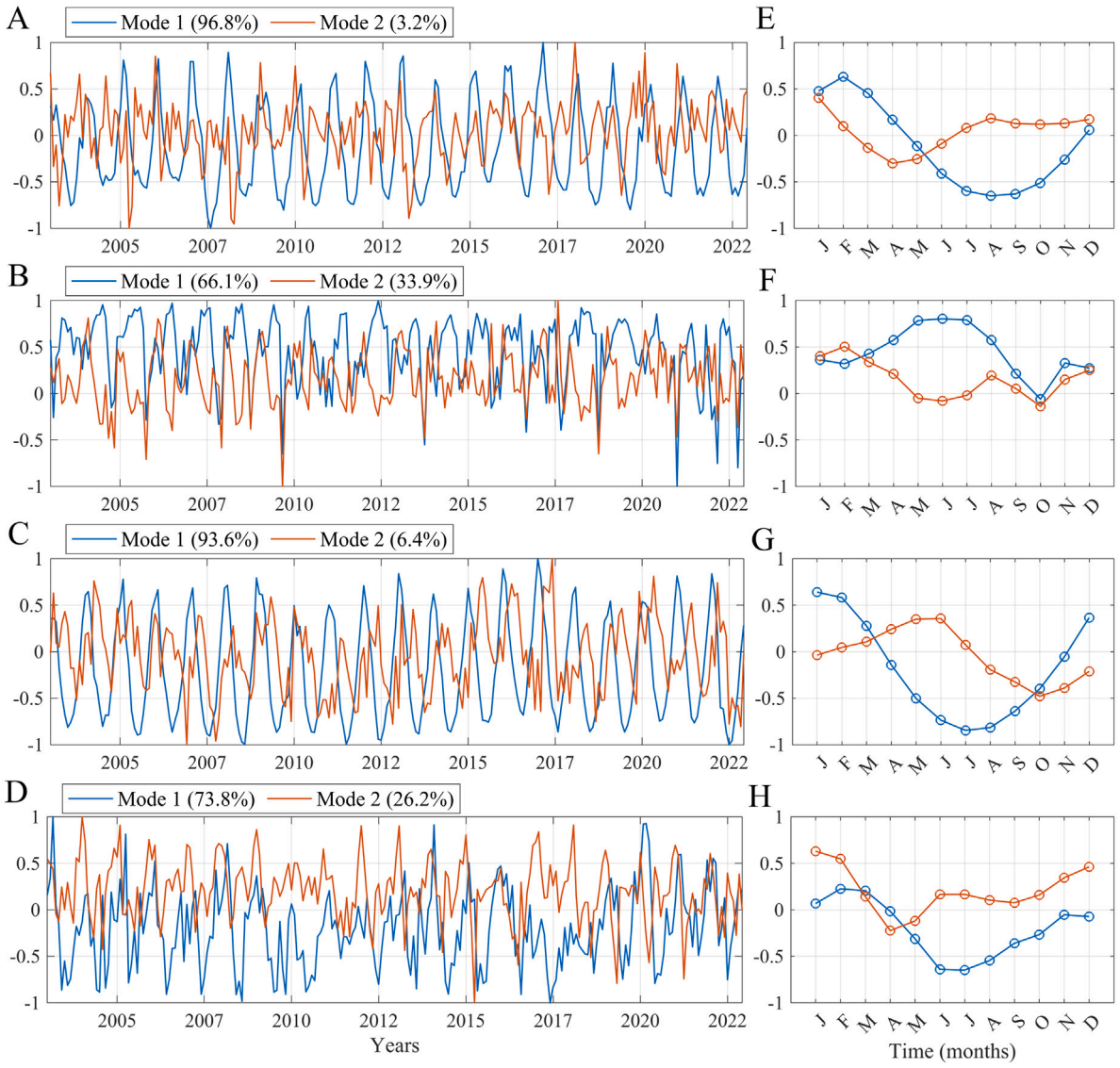

Fig. 3. Temporal dominant modes for SST and $nFLH$ in Tongoy Bay (A–B), and northern Chiloé (C–D). The temporal mode 1 (blue line), and mode 2 (orange line) are shown with their respective percentage of explained variance. The right panels show the climatological pattern for each mode. (For interpretation of the references to color in this figure legend, the reader is referred to the web version of this article.)

Multiple scale in synchrony in local bio-oceanographic characteristics

WC analyzes identified patterns of local environmental variability showing that, regardless of geographic distance, synchrony patterns between environmental processes were similar between Tongoy Bay and northern Chiloé. The PWC helped disentangle common dependencies and revealed differences in scale-specific relationships between both regions.

Temporal synchrony between $nFLH$ and SST in Tongoy Bay exhibited annual and, to some extent, semiannual synchrony throughout the study period. Furthermore, we observed transient periods of significant synchrony at the 2–3 yr band (Fig. 8A). When controlling for the effect of $ENSO$ through PWC the synchrony pattern was simplified (Fig. 8B), showing synchrony likely caused by the annual mode of $nFLH$. Synchrony between $nFLH$ and $ENSO$ (Fig. 8C) showed transients on sub-annual and inter-annual scale (2–6 yr). However, when controlled by SST, a significant period of multiscale coherence appears, the autotrophic biomass is more strongly associated with ENSO-related forcing (Fig. 8D).

In northern Chiloé, our analyzes revealed a similar pattern as described above for Tongoy: a marked annual synchronous signal between $nFLH$ and SST throughout the study period accompanied by annual synchrony (Fig. 9A). After excluding the effects of $ENSO$ the synchrony showed a significant annual pattern (Fig. 9B). The temporal co-occurrence between $nFLH$ and $ENSO$ showed scattered periods of synchrony at different scales across the study period (Fig. 9C). However, when controlling for SST, significant mode 2-3-year and 5–6-year appears and persists throughout the time series also highlights that multi-annual components are primarily influenced by ENSO (Fig. 9D).

4. Discussion

Using robust statistical methods, our results demonstrate that distinct biophysical modes of variability regulating shellfish productivity operate across multiple temporal and spatial scales. Previous research has largely emphasized the role of mesoscale to local processes in driving biophysical variability within our study regions. Among these drivers are coastal upwelling, river discharge under contrasting regimes (pluvial and/or nival), and nutrient inputs (Garreaud et al., 2011; Bravo et al., 2016; Garreaud, 2018; Flores et al., 2022), which may

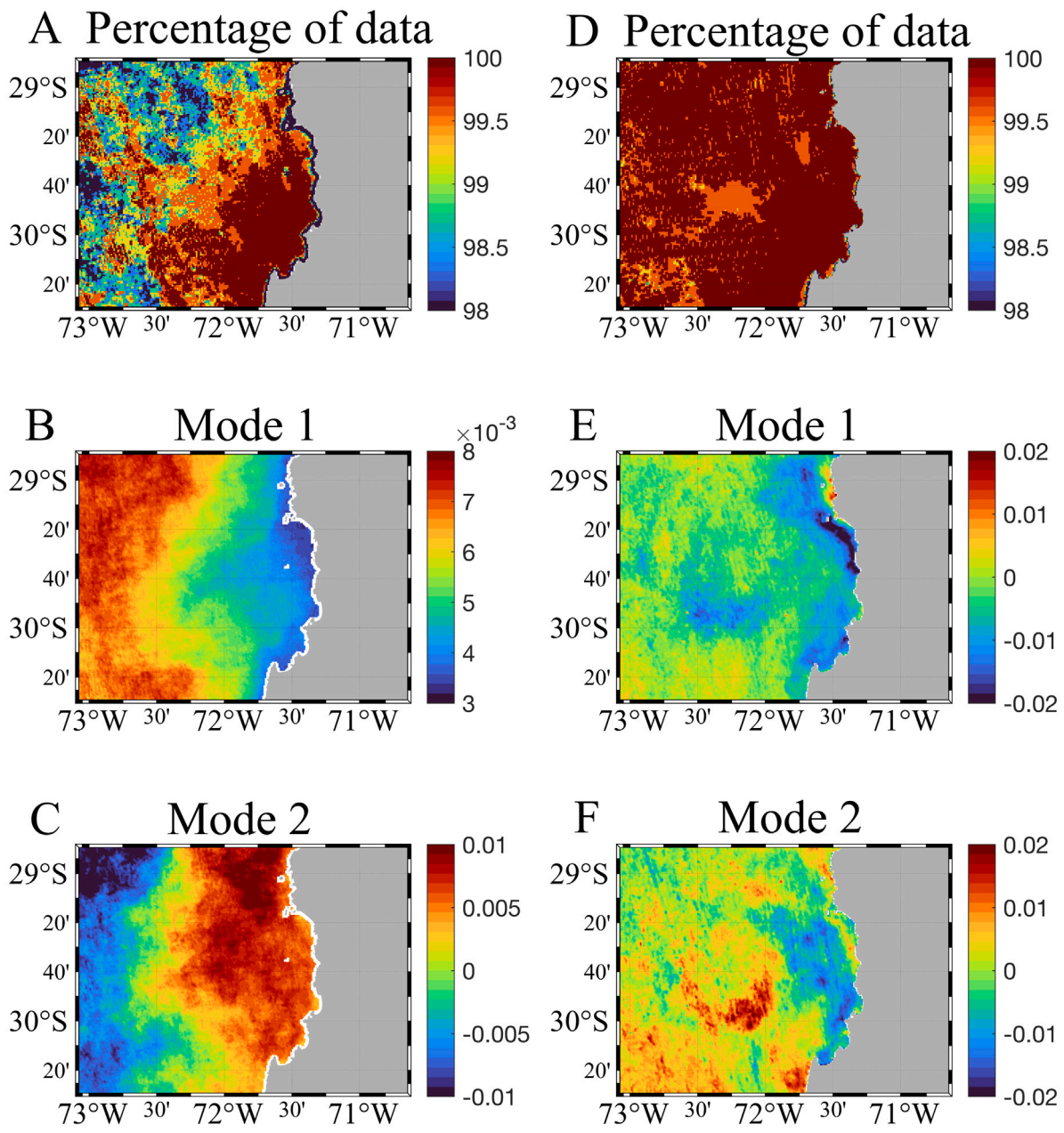

Fig. 4. (A) Percentage of data available for first and two EOF modes of SST in Tongoy Bay. (B) Space first mode of SST in Tongoy Bay. (C) Space second mode of SST in Tongoy Bay. (D) Percentage of data available for first two EOF modes of $nFLH$ in Tongoy Bay. (E) Space first mode of $nFLH$ in Tongoy Bay. (F) Space second mode of $nFLH$ in Tongoy Bay.

be associated with the variance captured by intra-seasonal scale (mode 2) of both SST and $nFLH$. However, a recent study Saavedra et al. (2020) synthesized the influence of multiple environmental drivers on coastal areas used for shellfish aquaculture in Chile and highlighted the complexity of interactions across different temporal and spatial scales. The authors demonstrated that distinct temporal modes of co-variability drive local environmental conditions, and that these conditions vary systematically along the latitudinal gradient. In this way, our results are a first step to address the complexity of the relationships between large-scale climatic forcing and mesoscale to local processes when evaluating the environmental context of aquaculture systems. The cross-scale relationship is manifested in the latitudinal contrast between regions. For example, coastal upwelling is a key driver of SST and $nFLH$. Yet persistent upwelling in northern Chile transitions to a distinctly seasonal upwelling regime in the south-central region (Blanco et al., 2001; Sobarzo et al., 2007; Narváez et al., 2019), and the latitudinal change is accompanied by the distinct change in the annual cycle in solar heat flux and light availability towards higher latitudes, which are synchronous with SST (Jacques-Coper et al., 2023). In contrast, $nFLH$ also exhibits an annual cycle, but the seasonal partitioning is less clear at higher latitudes, with a larger fraction of its variance is explained by the second mode in northern Chiloé. These results suggest that, although the annual cycle dominates the temporal evolution of the leading modes, local drivers — such as freshwater discharge — can generate regional variability in the spatial and temporal patterns of $nFLH$, particularly at higher latitudes. In northern Chiloé, phytoplankton biomass variability is modulated by nutrient availability (González et al., 2010), water column stratification and wind dynamics (Muñoz et al., 2023). The phytoplankton community in this region is largely dominated by diatoms (Montero et al., 2017), whose growth is closely associated with surface silicate concentration and enhanced stratification driven by freshwater input from rivers,

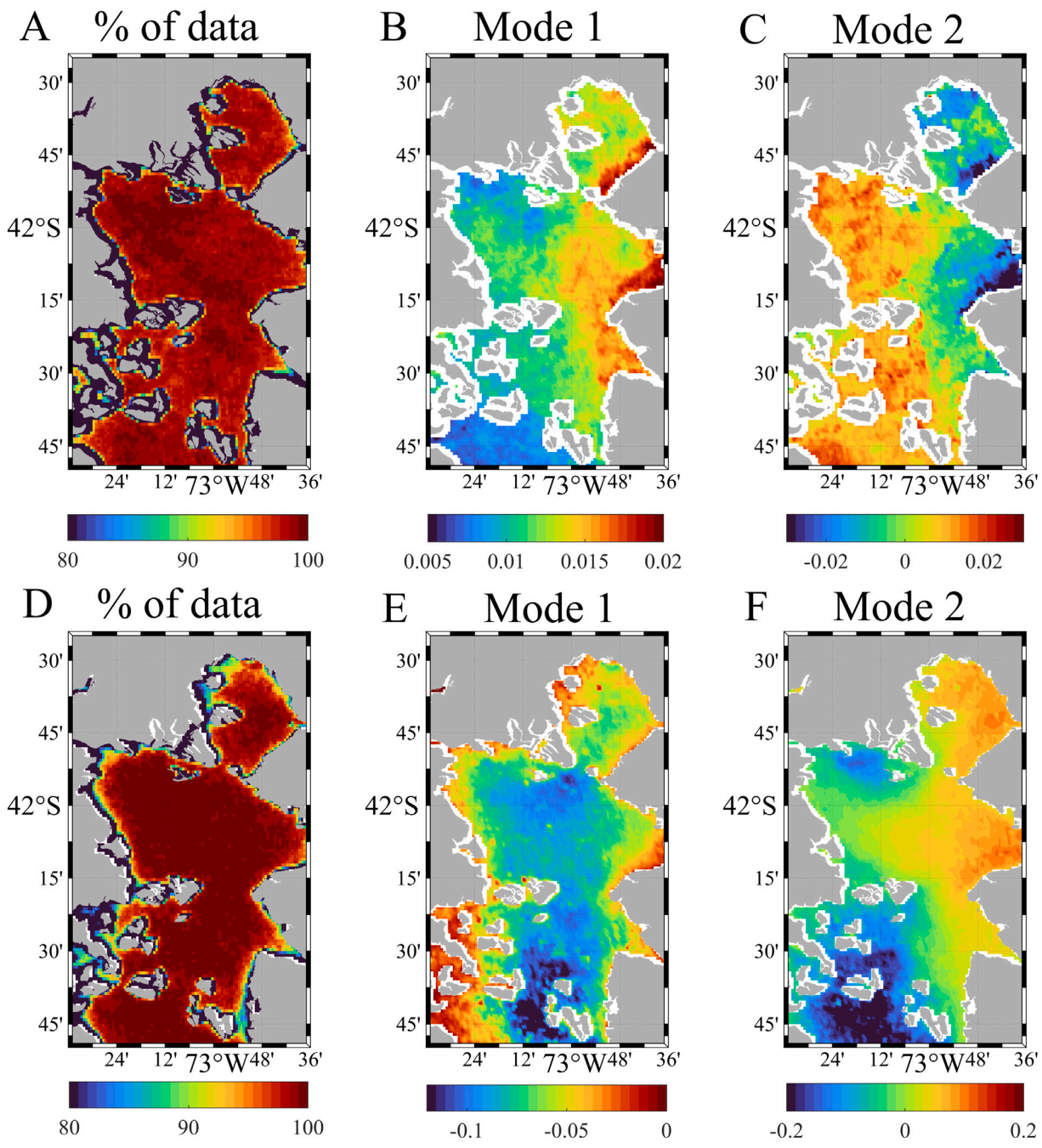

Fig. 5. (A) Percentage of data available for first and two EOF modes of SST in northern Chiloé. (B) Space first mode of SST in northern Chiloé. (C) Space second mode of SST in northern Chiloé. (D) Percentage of data available for first two EOF modes of $nFLH$ in northern Chiloé. (E) Space first mode of $nFLH$ in northern Chiloé. (F) Space second mode of $nFLH$ in northern Chiloé.

estuaries, and fjords (Cuevas et al., 2019). In contrast, in Tongoy Bay, nutrient availability for phytoplankton is primarily regulated by seasonally variable coastal upwelling events (Broitman et al., 2022). The spatial and temporal variability of $nFLH$, as revealed by EOF analysis, highlights the role of local forcing and physical processes in contributing to the variability captured by mode 2 and its associated fraction of the total variance (Iriarte et al., 2007; Cuevas et al., 2019; Moraga-Opazo et al., 2011).

Along the central and northern of Chile, the coastal zone is characterized by elevated biological productivity fueled by semipermanent upwelling (Montecino and Lange, 2009; Chavez and Messié, 2009). Tongoy Bay exhibits low seasonal and intraseasonal variability in SST, a condition associated with year-round upwelling (Fernández et al., 2024). At the local scale, energy fluxes are primarily driven by semidiurnal tides (Bravo et al., 2013). Hence, a local interaction of upwelling and tides may play a crucial role in the strongly seasonal transport of larvae to the coast over different seasonal periods. For example, larval delivery of benthic invertebrates, cultivated and wild is strongly seasonal (Broitman et al., 2022; Navarrete et al., 2022). In this way, beyond large-scale forcing, biophysical variability is dominated by mesoscale processes mainly accounted by subtle change to coastline topography and bathymetry. The dominant factors shaping biological activity in northern Patagonia, on the other hand, are vast; they include freshwater and terrigenous organic carbon inputs, and a complex coastline, which results in high spatial heterogeneity of local environmental conditions (González et al., 2013). Thus, autotrophic activity is

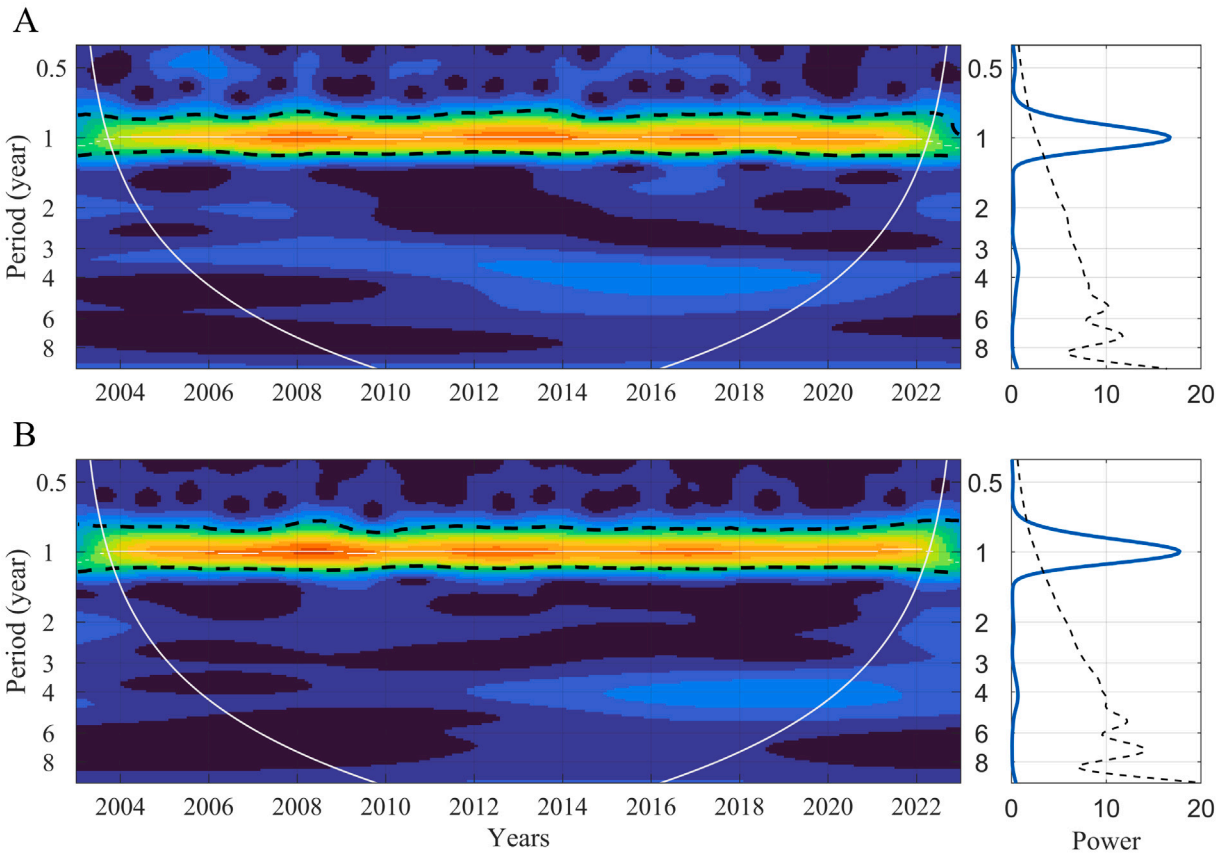

Fig. 6. Wavelet Power Spectrum (WPS) showing the dominant periods (in years) of variability for the SST 2003–2022 time series in (A) Tongoy Bay and (B) Northern Chiloé. The white line define the cone of influence above which computations are not influenced by edge effects. The color code for spectral power values is graded from blue (low power) to yellow (high power). The black dot-dashed lines indicate the 95% significant areas obtained by adapted bootstrapping (Cazelles et al., 2014). (For interpretation of the references to color in this figure legend, the reader is referred to the web version of this article.)

regulated by different physicochemical, environmental and biological factors; temperature, salinity, pH, turbidity, macronutrient availability, solar radiation, wind stress and grazing pressure (Poblete-Ulloa et al., 2024). Most of these factors, in turn, are driven primarily by the mixing of freshwater inputs from rivers, glacial melt, and heavy precipitation, together with the influx of Subantarctic Water and Equatorial SubSurface Water from the adjacent oceanic zone (Sievers and Silva, 2006; Linford et al., 2023).

Understanding the concurrent correlation scales between time series is essential for uncovering the underlying significance of synchrony patterns between large-scale climatic variability and local-scale environmental dynamics (Chavez and Cazelles, 2019). In this study, we selected two regions with contrasting environmental regimes, where functional relationships among environmental conditions may nonetheless be differentially affected by climate variability. According to various climate projections, a poleward shift of upwelling-favorable winds could disrupt the synchrony in the seasonal timing of local responses to global forcing. Along the Humboldt Current Ecosystem, complex responses such as shifts in the amplitude and timing of wind-driven coastal upwelling have already been observed (Aguirre et al., 2018). Although an intensification of upwelling is projected for the southern region, a weakening in seasonality at lower latitude may affect primary productivity (Du et al., 2024), potentially impacting the provision of key ecosystem services for aquaculture (Bograd et al., 2023; Du et al., 2024). A recent study demonstrated that the seasonality of larval arrival in two benthic species along the central-northern coast of Chile is modulated by the seasonal migration of the Southeastern Pacific Anticyclone, underscoring the complexity of coastal system responses to anthropogenic climate change (Navarrete et al., 2022; Weidberg et al., 2020). Likewise, detecting changes in phytoplankton phenology (for example, timing of initiation, peak biomass, and seasonal duration) provides critical insights into how climate-driven variability can affect trophic energy transfer to higher levels, carbon sequestration efficiency, and overall ecosystem functioning (Nicholson et al., 2025). It is worth emphasizing that our results reveal multiscale responses in environmental synchrony across both central-northern and southern Chile. These responses—manifested as changes in the co-variation between phytoplankton biomass (measured as FLH) and local SST can be interpreted as signatures of large-scale climatic forcing. Long-term climatic patterns and their impacts on hydrological conditions and biodiversity in northern Patagonia have been previously documented. The supply of mussel larvae to the aquaculture industry was disrupted, probably due to a decrease in the food availability for larvae, potentially driven by large-scale climatic variability (Lara et al., 2016). A positive phase synchrony between $ENSO$ and the Southern Annular Mode (SAM) led to anomalous local conditions, including reduced river discharge and diminished nutrient input from the adjacent ocean.

The Southeast Pacific Anticyclone (SPA) plays a key role in modulating atmospheric and oceanographic conditions along the southeastern Pacific. Its seasonal displacement and intensity regulate wind regimes, which in turn control coastal upwelling events and associated productivity (Schneider et al., 2017; Ancapichún and Garcés-Vargas, 2015). Interannual and decadal fluctuations in SPA are strongly linked to large-scale climate modes such as $ENSO$ and PDO (Aguirre et al., 2018; Muñoz et al., 2023). During El Niño events, which support high biological productivity in central–northern Chile (Broitman et al., 2022). Furthermore, a more complex synchrony in environmental and climatic variability is observed in the north Patagonian region (Lara

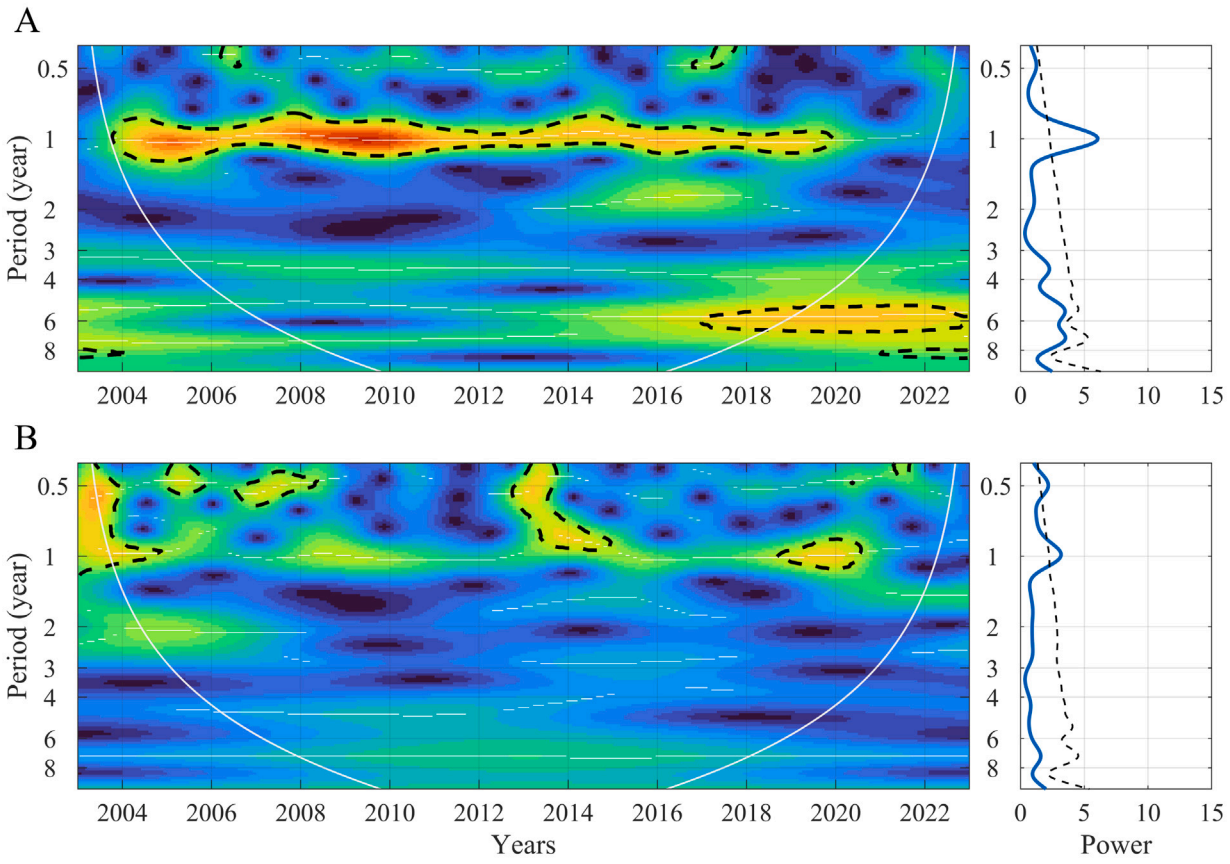

Fig. 7. Wavelet Power Spectrum (WPS) showing the dominant periods (in years) of variability for the $nFLH$ 2003–2022 time series in (A) Tongoy Bay, and (B) Northern Chiloé. The white line define the cone of influence above which computations are not influenced by edge effects. The color code for power values is graded from blue (low power) to yellow (high power). The black dot-dashed lines indicate the 95% significant areas obtained by adapted bootstrapping (Cazelles et al., 2014). (For interpretation of the references to color in this figure legend, the reader is referred to the web version of this article.)

et al., 2019b), where additionally, the poleward SPA migration contributed to the intensification of upwelling along the outer coast of the northern Patagonian fjords (Narváez et al., 2019; Pérez-Santos et al., 2019).

Bivalve aquaculture, including scallops and mussels along the Chilean coast, is highly dependent on larval supply from the environment. This intrinsic dependence makes the system particularly vulnerable to the impacts of climate change. Oceanographic features such as stratification and fronts, which form in response to warming or freshwater input, can act as barriers to larval dispersal (Woodson and Litvin, 2015). However, these structures may be disrupted by storms, suggesting that climate change could influence the availability of bivalve larvae. On the other hand, temperature is a key factor that regulates shellfish growth (Almada-Villela et al., 1982): it affects metabolism, food conversion efficiency, energy expenditure, and oxygen demand (Matoo et al., 2021). Moderate temperature increases within a species physiological tolerance can enhance growth, but exceeding this range results in reduced growth and feeding, increased mortality, and deterioration in flesh quality. Our results suggest that SST variability in shellfish habitats is driven by large-scale temporal and spatial forcing, including $ENSO$ dynamics, which has differential impacts between shellfish production regions. Global warming is projected to increase the frequency and intensity of $ENSO$ events, alter the complexity of their atmospheric teleconnections, and increase the likelihood of more severe El Niño occurrences (Chen et al., 2024). Based on our findings, these changes can alter the suitability of shellfish habitats, affecting organism physiology and the viability of aquaculture operations.

5. Conclusion

The transition from free-swimming larvae to juvenile stages represents a critical bottleneck in the production of viable individuals for aquaculture. Climate-induced changes — such as fluctuations in sea surface temperature and shifts in the availability of larval food — pose significant risks to the physiological performance and survival of farmed species. These environmental perturbations can modify the spatial and temporal distribution of marine organisms, particularly those of commercial importance, with potentially profound consequences for food security.

In both Tongoy Bay and northern Chiloé, our results demonstrate that large-scale climatic variability exerts a dominant influence on the synchrony of key oceanographic characteristics derived from satellite observations, thereby shaping the local environmental dynamics of coastal ecosystems. The temporal evolution of autotrophic biomass was largely governed by the annual cycle of SST, reflecting the central role of temperature in structuring productivity. Moreover, differences in the magnitude and timing of synchrony between oceanographic variables in the two shellfish-farming regions were associated with the influence of large-scale $ENSO$ variability acting across multiple temporal scales. These findings underscore that shellfish productivity depends on the multiscale interplay between climatic and local forcing, which constrains the predictability of environmental conditions. Ultimately, this study highlights the value of identifying the temporal windows and scales of environmental synchrony as a basis for developing adaptive management strategies that better integrate ecological dynamics with climatic variability across spatial and temporal gradients.

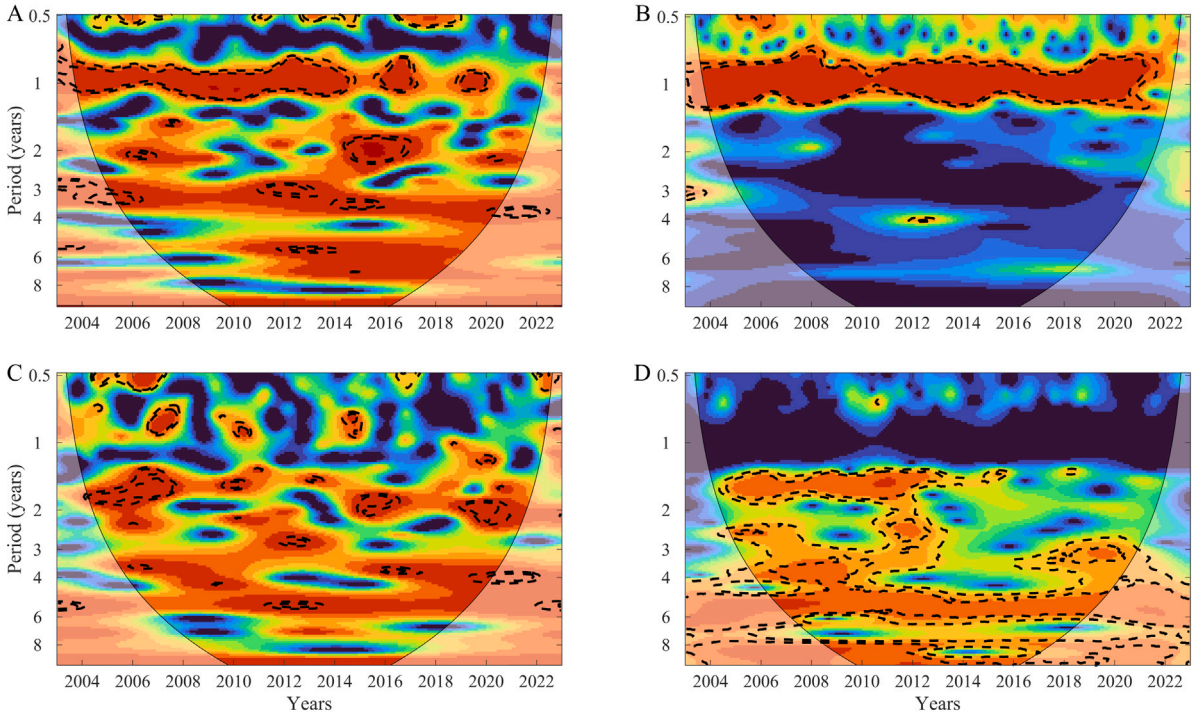

Fig. 8. Wavelet Coherence and Partial Wavelet Coherence in Tongoy Bay. (A) Wavelet Coherence between $nFLH$ and SST. (B) Partial Wavelet Coherence between $nFLH$ and SST controlled $ENSO$. (C) Wavelet Coherence between $nFLH$ and $ENSO$. (D) Partial Wavelet Coherence between $nFLH$ and $ENSO$ controlled by SST. The black line define the cone of influence above which computations are not influenced by edge effects. The color code for coherence values is graded from blue (low synchrony) to yellow (high synchrony). The black dot-dashed lines indicate the 95% and 90% significant areas obtained by adapted bootstrapping (Cazelles et al., 2014). (For interpretation of the references to color in this figure legend, the reader is referred to the web version of this article.)

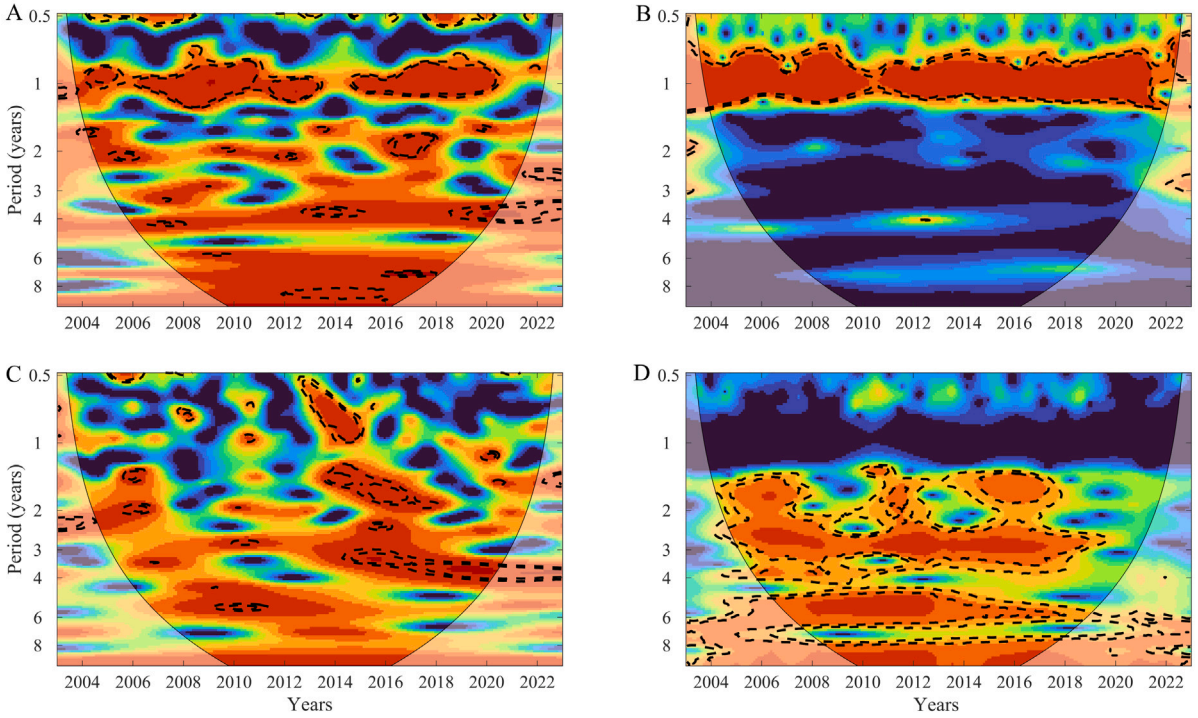

Fig. 9. Wavelet Coherence and Partial Wavelet Coherence in Northern Chiloé. (A) Wavelet Coherence between $nFLH$ and SST. (B) Partial Wavelet Coherence between $nFLH$ and SST controlled $ENSO$. (C) Wavelet Coherence between $nFLH$ and $ENSO$. (D) Partial Wavelet Coherence between $nFLH$ and $ENSO$ controlled by SST. The black line define the cone of influence above which computations are not influenced by edge effects. The color code for coherence values is graded from blue (low synchrony) to yellow (high synchrony). The black dot-dashed lines indicate the 95% and 90% significant areas obtained by adapted bootstrapping (Cazelles et al., 2014). (For interpretation of the references to color in this figure legend, the reader is referred to the web version of this article.)

CRediT authorship contribution statement

Carlos Lara: Writing – review & editing, Writing – original draft, Investigation, Funding acquisition, Formal analysis, Data curation, Conceptualization. **Richard Muñoz:** Writing – review & editing, Writing – original draft, Methodology, Formal analysis, Data curation. **Sebastián I. Vásquez:** Writing – review & editing, Writing – original draft, Methodology, Data curation. **Felipe I. Torres:** Writing – review & editing, Writing – original draft, Methodology, Investigation, Formal analysis. **Amalia M.S. Detoni:** Writing – review & editing, Writing – original draft, Investigation, Formal analysis. **Bernardo R. Broitman:** Writing – review & editing, Writing – original draft, Methodology, Investigation, Funding acquisition, Conceptualization. **Bernard Cazelles:** Writing – review & editing, Writing – original draft, Visualization, Validation, Software, Methodology, Investigation, Formal analysis, Data curation, Conceptualization.

Declaration of competing interest

The authors declare that they have no known competing financial interests or personal relationships that could have appeared to influence the work reported in this paper.

Acknowledgments

This study was partially supported by FONDECYT 1230420 and Dirección de Investigación at the Universidad Católica de la Santísima Concepción FAA 2025 to C.L. R.M. and S.I.V. were supported by the Chilean National Research and Development Agency (ANID) through doctoral grants 21231834 and 21221020, respectively. B.R.B. was supported by FONDECYT 1221699 and Instituto Milenio SECOS (ICN2019-015). MODIS data is available at NASA's ocean color website. http://oceancolor.gsfc.nasa.gov.

Data availability

Data will be made available on request.

References

Abbate, M.C.L., Molinero, J.C., Guinder, V.A., Perillo, G.M., Freije, R.H., Sommer, U., Spetter, C.V., Marcovecchio, J.E., 2017. Time-varying environmental control of phytoplankton in a changing estuarine system. Sci. Total Environ. 609, 1390–1400.

Aguirre, C., García-Loyola, S., Testa, G., Silva, D., Farías, L., 2018. Insight into anthropogenic forcing on coastal upwelling off south-central Chile. Elementa Sci. the Anthopocene 6, 59.

Almada-Villela, P.C., Davenport, J., Gruffydd, L.D., 1982. The effects of temperature on the shell growth of young mytilus edulis l.. J. Exp. Mar. Biology Ecol. 59 (2–3), 275–288.

Ancapichún, S., Garcés-Vargas, J., 2015. Variability of the southeast Pacific subtropical anticyclone and its impact on sea surface temperature off north-central Chile. Cienc. Mar. 41 (1), 1–20.

Bakit, J., Hurtado, A., Márquez, R., Villasante, S., 2023. Navigating transformations from artisanal fishers to entrepreneurial scallop farmers in Chile. Front. Mar. Sci. 10, 1128527.

Barrows, T.T., Juggins, S., De Deckker, P., Calvo, E., Pelejero, C., 2007. Long-term sea surface temperature and climate change in the Australian–New Zealand region. Paleoceanography 22 (2).

Batchelder, H.P., Mackas, D.L., O'Brien, T.D., 2012. Spatial–temporal scales of synchrony in marine zooplankton biomass and abundance patterns: a world-wide comparison. Prog. Oceanogr. 97, 15–30.

Behrenfeld, M.J., Westberry, T.K., Boss, E., O'Malley, R.T., Siegel, D.A., Wiggert, J.D., Franz, B., McClain, C., Feldman, G., Doney, S.C., et al., 2009. Satellite-detected fluorescence reveals global physiology of ocean phytoplankton. Biogeosciences 6 (5), 779–794.

Bjørnstad, O.N., Ims, R.A., Lambin, X., 1999. Spatial population dynamics: analyzing patterns and processes of population synchrony. Trends Ecol. Evolut. 14 (11), 427–432.

Blanco, J., Thomas, A., Carr, M.-E., Strub, P.T., 2001. Seasonal climatology of hydrographic conditions in the upwelling region off northern Chile. J. Geophys. Res.: Ocean. 106 (C6), 11451–11467.

Bograd, S.J., Jacox, M.G., Hazen, E.L., Lovecchio, E., Montes, I., Pozo Buil, M., Shannon, L.J., Sydeman, W.J., Rykaczewski, R.R., 2023. Climate change impacts on eastern boundary upwelling systems. Annu. Rev. Mar. Sci. 15 (1), 303–328.

Boyd, C.E., McNevin, A.A., Davis, R.P., 2022. The contribution of fisheries and aquaculture to the global protein supply. Food Secur. 14 (3), 805–827.

von Brand, E., Abarca, A., Merino, G.E., Stotz, W., 2016. Scallop fishery and aquaculture in Chile: A history of developments and declines. In: Developments in Aquaculture and Fisheries Science. vol. 40, Elsevier, pp. 1047–1072.

Bravo, L., Ramos, M., Astudillo, O., Dewitte, B., Goubanova, K., 2016. Seasonal variability of the ekman transport and pumping in the upwelling system off central-northern Chile (30°s) based on a high-resolution atmospheric regional model (WRF). Ocean. Sci. 12 (5), 1049–1065.

Bravo, L., Ramos, M., Sobarzo, M., Pizarro, O., Valle-Levinson, A., 2013. Barotropic and baroclinic semidiurnal tidal currents in two contrasting coastal upwelling zones of Chile. J. Geophys. Res.: Ocean. 118 (3), 1226–1238.

Broitman, B.R., Halpern, B.B.S., Gelcich, S., Lardies, M.A.M., Vargas, C.A.C., Vásquez-Lavín, F., Widdicombe, S., Birchenough, S.N.S., 2017. Dynamic interactions among boundaries and the expansion of sustainable aquaculture. Front. Mar. Sci. 4, 2–5. http://dx.doi.org/10.3389/fmars.2017.00015.

Broitman, B.R., Lara, C., Flores, R.P., Saldías, G.S., Piñones, A., Pinochet, A., Mejía, A.G., Navarrete, S.A., 2022. Environmental variability and larval supply to wild and cultured shellfish populations. Aquaculture 548, 737639.

Buttay, L., Cazelles, B., Miranda, A., Casas, G., Nogueira, E., González-Quirós, R., 2017. Environmental multi-scale effects on zooplankton inter-specific synchrony. Limnol. Oceanogr. 62 (4), 1355–1365.

Cazelles, B., 2004. Symbolic dynamics for identifying similarity between rhythms of ecological time series. Ecol. Lett. 7 (9), 755–763.

Cazelles, B., Cazelles, K., Chavez, M., 2014. Wavelet analysis in ecology and epidemiology: impact of statistical tests. J. R. Soc. Interface 11 (91), 20130585.

Cazelles, B., Cazelles, K., Tian, H., Chavez, M., Pascual, M., 2023. Disentangling local and global climate drivers in the population dynamics of mosquito-borne infections. Sci. Adv. 9 (39), eadf7202.

Cazelles, B., Chavez, M., Berteaux, D., Ménard, F., Vik, J.O., Jenouvrier, S., Stenseth, N.C., 2008. Wavelet analysis of ecological time series. Oecologia 156, 287–304.

Cazelles, B., Chavez, M., Magny, G.C.d., Guégan, J.-F., Hales, S., 2007. Time-dependent spectral analysis of epidemiological time-series with wavelets. J. R. Soc. Interface 4 (15), 625–636.

Cazelles, B., Stone, L., 2003. Detection of imperfect population synchrony in an uncertain world. J. Anim. Ecol. 72, 953–968.

Chavez, M., Cazelles, B., 2019. Detecting dynamic spatial correlation patterns with generalized wavelet coherence and non-stationary surrogate data. Sci. Rep. 9 (1), 7389.

Chavez, F.P., Messié, M., 2009. A comparison of Eastern Boundary Upwelling Ecosystems. Prog. Oceanogr. 83 (1–4), 80–96.

Chen, Z., Li, L., Wang, B., Fan, J., Lu, T., Lv, K., 2024. The impact of global warming on ENSO from the perspective of objective signals. Atmos. Res. 299, 107176.

Cuevas, L.A., Tapia, F.J., Iriarte, J.L., González, H.E., Silva, N., Vargas, C.A., 2019. Interplay between freshwater discharge and oceanic waters modulates phytoplankton size-structure in fjords and channel systems of the Chilean patagonia. Prog. Oceanogr. 173, 103–113.

Defriez, E.J., Reuman, D.C., 2017a. A global geography of synchrony for marine phytoplankton. Glob. Ecol. Biogeogr. 26 (8), 867–877.

Defriez, E.J., Reuman, D.C., 2017b. A global geography of synchrony for terrestrial vegetation. Glob. Ecol. Biogeogr. 26 (8), 878–888.

Du, T., Wang, S., Jing, Z., Wu, L., Zhang, C., Zhang, B., 2024. Future changes in coastal upwelling and biological production in eastern boundary upwelling systems. Nat. Commun. 15 (1), 6238.

Duveiller, G., Forzieri, G., Robertson, E., Li, W., Georgievski, G., Lawrence, P., Wiltshire, A., Ciais, P., Pongratz, J., Sitch, S., et al., 2018. Biophysics and vegetation cover change: a process-based evaluation framework for confronting land surface models with satellite observations. Earth Syst. Sci. Data 10 (3), 1265–1279.

Ezgeta-Balić, D., Najdek, M., Peharda, M., Blažina, M., 2012. Seasonal fatty acid profile analysis to trace origin of food sources of four commercially important bivalves. Aquaculture 334, 89–100.

FAO, 2020. The state of world fisheries and aquaculture. sustainability in action. rome:Fao..

FAO, 2025. Global aquaculture production. URL https://www.fao.org/fishery/en/collection/aquaculture?lang=en.

Fernández, C., Poupin, M.J., Lagos, N.A., Broitman, B.R., Lardies, M.A., 2024. Physiological resilience of intertidal chitons in a persistent upwelling coastal region. Sci. Rep. 14 (1), 21401.

Ferreira, A., Sá, C., Silva, N., Beltrán, C., Dias, A., Brito, A., 2020. Phytoplankton response to nutrient pulses in an upwelling system assessed through a microcosm experiment (algarrobo bay, Chile). Ocean & Coastal Management 190, 105167.

Flores, R.P., Lara, C., Saldías, G.S., Vásquez, S.I., Roco, A., 2022. Spatio-temporal variability of turbid freshwater plumes in the inner sea of chiloé, northern patagonia. J. Mar. Syst. 228, 103709.

Froehlich, H.E., Gentry, R.R., Halpern, B.S., 2018. Global change in marine aquaculture production potential under climate change. Nat. Ecol. Evol. 2 (11), 1745–1750.

Garreaud, R., 2018. Record-breaking climate anomalies lead to severe drought and environmental disruption in western patagonia in 2016. Clim. Res. 74 (3), 217–229.

Garreaud, R.D., Rutllant, J.A., Muñoz, R.C., Rahn, D.A., Ramos, M., Figueroa, D., 2011. VOCALS-cupex: the Chilean upwelling experiment. Atmospheric Chem. Phys. 11 (5), 2015–2029.

Ghil, M., Allen, M.R., Dettinger, M.D., Ide, K., Kondrashov, D., Mann, M.E., Robertson, A.W., Saunders, A., Tian, Y., Varadi, F., et al., 2002. Advanced spectral methods for climatic time series. Rev. Geophys. 40 (1), 1–3.

González, H., Calderón, M., Castro, L., Clement, A., Cuevas, L., Daneri, G., Iriarte, J., Lizárraga, L., Martínez, R., Menschel, E., et al., 2010. Primary production and plankton dynamics in the reloncavífjord and the interior sea of chiloé, northern patagonia, Chile. Mar. Ecol. Prog. Ser. 402, 13–30.

González, H., Castro, L., Daneri, G., Iriarte, J., Silva, N., Tapia, F., Teca, E., Vargas, C., 2013. Land–ocean gradient in haline stratification and its effects on plankton dynamics and trophic carbon fluxes in Chilean patagonian fjords (47–50 °s). Prog. Oceanogr. 119, 32–47.

Hansen, B.B., Grøtan, V., Herfindal, I., Lee, A.M., 2020. The moran effect revisited: spatial population synchrony under global warming. Ecography 43 (11), 1591–1602.

Iriarte, J., González, H., Liu, K., Rivas, C., Valenzuela, C., 2007. Spatial and temporal variability of chlorophyll and primary productivity in surface waters of southern Chile (41.5–43 °s). Estuar. Coast. Shelf Sci. 74 (3), 471–480.

Jacques-Coper, M., Segura, C., de la Torre, M.B., Valdebenito Muñoz, P., Vásquez, S.I., Narváez, D.A., 2023. Synoptic-to-intraseasonal atmospheric modulation of phytoplankton biomass in the inner sea of chiloé, northwest patagonia (42.5°-43.5° s , 72.5°-74° w), Chile. Front. Mar. Sci. 10, 1160230.

Jiang, Z., Liu, J., Chen, J., Chen, Q., Yan, X., Xuan, J., Zeng, J., 2014. Responses of summer phytoplankton community to drastic environmental changes in the changjiang (yangtze river) estuary during the past 50 years. Water Res. 54, 1–11.

Kahru, M., Di Lorenzo, E., Manzano-Sarabia, M., Mitchell, B.G., 2012. Spatial and temporal statistics of sea surface temperature and chlorophyll fronts in the california current. J. Plankton Res. 34 (9), 749–760.

Lagos, N.A., Benítez, S., Duarte, C., Lardies, M.A., Broitman, B.R., Tapia, C., Tapia, P., Widdicombe, S., Vargas, C.A., 2016. Effects of temperature and ocean acidification on shell characteristics of argopecten purpuratus: implications for scallop aquaculture in an upwelling-influenced area. Aquac. Environ. Interactions 8, 357–370.

Lara, C., Cazelles, B., Saldías, G.S., Flores, R.P., Paredes, Á.L., Broitman, B.R., 2019a. Coupled biospheric synchrony of the coastal temperate ecosystem in northern patagonia: a remote sensing analysis. Remote. Sens. 11 (18), 2092.

Lara, C., Saldías, G.S., Cazelles, B., Rivadeneira, M.M., Haye, P.A., Broitman, B.R., 2019b. Coastal biophysical processes and the biogeography of rocky intertidal species along the south-eastern Pacific. J. Biogeogr. 46 (2), 420–431.

Lara, C., Saldías, G.S., Tapia, F.J., Iriarte, J.L., Broitman, B.R., 2016. Interannual variability in temporal patterns of chlorophyll–a and their potential influence on the supply of mussel larvae to inner waters in northern patagonia (41–44° s). J. Mar. Syst. 155, 11–18.

Linford, P., Pérez-Santos, I., Montes, I., Dewitte, B., Buchan, S., Narváez, D., Saldías, G., Pinilla, E., Garreaud, R., Díaz, P., et al., 2023. Recent deoxygenation of patagonian fjord subsurface waters connected to the peru–Chile undercurrent and equatorial subsurface water variability. Glob. Biogeochem. Cycles 37 (6), e2022GB007688.

Liu, Y., Wu, H., Wang, J., Long, M., 2022. Non-stationary transformers: Exploring the stationarity in time series forecasting. Adv. Neural Inf. Process. Syst. 35, 9881–9893.

Martinez, E., Antoine, D., D'Ortenzio, F., Gentili, B., 2009. Climate-driven basin-scale decadal oscillations of oceanic phytoplankton. Science 326 (5957), 1253–1256.

Matoo, O.B., Lannig, G., Bock, C., Sokolova, I.M., 2021. Temperature but not ocean acidification affects energy metabolism and enzyme activities in the blue mussel, mytilus edulis. Ecol. Evol. 11 (7), 3366–3379.

Maulu, S., Hasimuna, O.J., Haambiya, L.H., Monde, C., Musuka, C.G., Makorwa, T.H., Munganga, B.P., Phiri, K.J., Nsekanabo, J.D., 2021. Climate change effects on aquaculture production: sustainability implications, mitigation, and adaptations. Front. Sustain. Food Syst. 5, 609097.

Molinet, C., Soto, D., León-Muñoz, J., Díaz, M., Espinoza, K., Henríquez, J., Matamala, T., 2025. Climate-driven changes in freshwater inputs to a northern patagonia fjord and overfishing of wild mussel seed could threaten Chilean mussel farming. Clim. Change 178, 1–19. http://dx.doi.org/10.1007/S10584-025-03956-X/TABLES/1.

Montecino, V., Lange, C.B., 2009. The humboldt current system: Ecosystem components and processes, fisheries, and sediment studies. Prog. Oceanogr. 83 (1–4), 65–79.

Montero, P., Daneri, G., Tapia, F., Iriarte, J.L., Crawford, D., 2017. Diatom blooms and primary production in a channel ecosystem of central patagonia. Lat. Am. J. Aquat. Res. 45 (5), 999–1016.

Moraga-Opazo, J., Valle-Levinson, A., Ramos, M., Pizarro-Koch, M., 2011. Upwelling-triggered near-geostrophic recirculation in an equatorward facing embayment. Cont. Shelf Res. 31 (19–20), 1991–1999.

Muñoz, R., Vergara, O.A., Figueroa, P.A., Mardones, P., Sobarzo, M., Saldías, G.S., 2023. On the phenology of coastal upwelling off central-southern Chile. Dyn. Atmos. Oceans 104, 101405.

Narváez, D.A., Vargas, C.A., Cuevas, L.A., García-Loyola, S.A., Lara, C., Segura, C., Tapia, F.J., Broitman, B.R., 2019. Dominant scales of subtidal variability in coastal hydrography of the northern Chilean patagonia. J. Mar. Syst. 193, 59–73.

Navarrete, S.A., Barahona, M., Weidberg, N., Broitman, B.R., 2022. Climate change in the coastal ocean: shifts in pelagic productivity and regionally diverging dynamics of coastal ecosystems. Proc. R. Soc. B 289 (1970), 20212772.

Newell, C.R., Hawkins, A.J., Morris, K., Boss, E., Thomas, A.C., Kiffney, T.J., Brady, D.C., 2021. Using high-resolution remote sensing to characterize suspended particulate organic matter as bivalve food for aquaculture site selection. J. Shellfish. Res. 40, 113–118. http://dx.doi.org/10.2983/035.040.0110.

Nicholson, S.-A., Ryan-Keogh, T.J., Thomalla, S.J., Chang, N., Smith, M.E., 2025. Satellite-derived global-ocean phytoplankton phenology indices. Earth Syst. Sci. Data 17 (5), 1959–1975.

O'Reilly, J.E., Maritorena, S., Siegel, D.A., O'Brien, M.C., Toole, D., Mitchell, B.G., Kahru, M., Chavez, F.P., Strutton, P., Cota, G.F., et al., 2000. Ocean color chlorophyll a algorithms for SeaWiFS, OC2, and OC4: Version 4. SeaWiFS Postlaunch Calibration Valid. Anal. Part 3, 9–23.

Ottinger, M., Clauss, K., Kuenzer, C., 2016. Aquaculture: Relevance, distribution, impacts and spatial assessments–a review. Ocean & Coastal Management 119, 244–266.

Pérez-Santos, I., Seguel, R., Schneider, W., Linford, P., Donoso, D., Navarro, E., Amaya-Cárcamo, C., Pinilla, E., Daneri, G., 2019. Synoptic-scale variability of surface winds and ocean response to atmospheric forcing in the eastern austral Pacific ocean. Ocean. Sci. 15 (5), 1247–1266.

Philippart, C.J., van Aken, H.M., Beukema, J.J., Bos, O.G., Cadée, G.C., Dekker, R., 2003. Climate-related changes in recruitment of the bivalve macoma balthica. Limnol. Oceanogr. 48 (6), 2171–2185.

Poblete-Ulloa, J., Gutiérrez, M.H., Lange, C.B., Narváez, D.A., Montero, P., González, H.E., Fernández, C., 2024. Freshwater discharge drives latitudinal changes of phytoplankton composition on the continental shelf off Chilean patagonia. J. Mar. Syst. 103993.

Ramajo, L., Valladares, M., Astudillo, O., Fernández, C., Rodríguez-Navarro, A.B., Watt-Arévalo, P., nez, M.N., Grenier, C., Román, R., Aguayo, P., Lardies, M.A., Broitman, B.R., Tapia, P., Tapia, C., 2020. Upwelling intensity modulates the fitness and physiological performance of coastal species: Implications for the aquaculture of the scallop argopecten purpuratus in the humboldt current system. Sci. Total Environ. 745, 140949. http://dx.doi.org/10.1016/j.scitotenv.2020.140949.

Reid, G.K., Gurney-Smith, H.J., Flaherty, M., Garber, A.F., Forster, I., Brewer-Dalton, K., Knowler, D., Marcogliese, D.J., Chopin, T., Moccia, R.D., et al., 2019. Climate change and aquaculture: considering adaptation potential. Aquac. Environ. Interactions 11, 603–624.

Saavedra, L.M., Saldías, G.S., Broitman, B.R., Vargas, C.A., 2020. Carbonate chemistry dynamics in shellfish farming areas along the Chilean coast: natural ranges and biological implications. ICES J. Mar. Sci. 78 (1), 323–339.

Saldías, G.S., Hernández, W., Lara, C., Muñoz, R., Rojas, C., Vásquez, S., Pérez-Santos, I., Soto-Mardones, L., 2021. Seasonal variability of SST fronts in the inner sea of chiloé and its adjacent coastal ocean, northern patagonia. Remote. Sens. 13 (2), 181.

Schneider, W., Donoso, D., Garcés-Vargas, J., Escribano, R., 2017. Water-column cooling and sea surface salinity increase in the upwelling region off central-south Chile driven by a poleward displacement of the south Pacific high. Prog. Oceanogr. 151, 38–48.

Sheppard, L.W., Defriez, E.J., Reid, P.C., Reuman, D.C., 2019. Synchrony is more than its top-down and climatic parts: interacting moran effects on phytoplankton in british seas. PLoS Comput. Biol. 15 (3), e1006744.

Sievers, H.A., Silva, N., 2006. Masas de agua y circulación en los canales y fiordos australes. Av. En El Conoc. Oceanográfico de Las Aguas Interiores Chil. Puerto Montt A Cabo de Hornos. ComitÉ Oceanográfico Nacional-Pontificia Univ. Católica de ValparaíSo, ValparaíSo 53–58.

Snyder, J., Boss, E., Weatherbee, R., Thomas, A.C., Brady, D., Newell, C., 2017. Oyster aquaculture site selection using landsat 8-derived sea surface temperature, turbidity, and chlorophyll a. Front. Mar. Sci. 4, 190. http://dx.doi.org/10.3389/fmars.2017.00190, URL http://journal.frontiersin.org/article/10.3389/fmars.2017.00190/full.

Sobarzo, M., Bravo, L., Donoso, D., Garcés-Vargas, J., Schneider, W., 2007. Coastal upwelling and seasonal cycles that influence the water column over the continental shelf off central Chile. Prog. Oceanogr. 75 (3), 363–382.

Stramski, D., Joshi, I., Reynolds, R.A., 2022. Ocean color algorithms to estimate the concentration of particulate organic carbon in surface waters of the global ocean in support of a long-term data record from multiple satellite missions. Remote Sens. Environ. 269, 112776.

Sundararaman, H.K.K., Shanmugam, z., 2024. Estimates of the global ocean surface dissolved oxygen and macronutrients from satellite data. Remote Sens. Environ. 311, 114243.

Thackeray, S.J., Sparks, T.H., Frederiksen, M., Burthe, S., Bacon, P.J., Bell, J.R., Botham, M.S., Brereton, T.M., Bright, P.W., Carvalho, L., et al., 2010. Trophic level asynchrony in rates of phenological change for marine, freshwater and terrestrial environments. Global Change Biol. 16 (12), 3304–3313.

Thomson, R.E., Emery, W.J., 2014. Data Analysis Methods in Physical Oceanography. Newnes.

Torres, F.I., Lara, C., Sillero, N., Broitman, B.R., 2025. Climate-induced habitat shifts of farmed mussel species. Aquaculture 742304.

Tsang, T.P., Ponisio, L.C., Bonebrake, T.C., 2023. Increasing synchrony opposes stabilizing effects of species richness on terrestrial communities. Diversity and Distributions 29 (7), 849–861.

Walter, J.A., Emery, K.A., Dugan, J.E., Hubbard, D.M., Bell, T.W., Sheppard, L.W., Karatayev, V.A., Cavanaugh, K.C., Reuman, D.C., Castorani, M.C., 2024. Spatial synchrony cascades across ecosystem boundaries and up food webs via resource subsidies. Proc. Natl. Acad. Sci. 121 (2), e2310052120.

Wanner, M.S., Walter, J.A., Reuman, D.C., Bell, T.W., Castorani, M.C., 2024. Dispersal synchronizes giant kelp forests. Ecology e4270.

Weidberg, N., Ospina-Alvarez, A., Bonicelli, J., Barahona, M., Aiken, C.M., Broitman, B.R., Navarrete, S.A., 2020. Spatial shifts in productivity of the coastal ocean over the past two decades induced by migration of the Pacific anticyclone and bakun's effect in the humboldt upwelling ecosystem. Glob. Planet. Change 193, 103259.

Woodson, C.B., Litvin, S.Y., 2015. Ocean fronts drive marine fishery production and biogeochemical cycling. Proc. Natl. Acad. Sci. 112 (6), 1710–1715.

Xiao, X., He, J., Yu, Y., Cazelles, B., Li, M., Jiang, Q., Xu, C., 2019. Teleconnection between phytoplankton dynamics in north temperate lakes and global climatic oscillation by time-frequency analysis. Water Res. 154, 267–276.